EEE 6505 | Nanophotonics and Plasmonics | April 2021 | Final Report

Review on the physics and application of sub-wavelength holes on metal films

Shadman Shahid, Rizwan Sheikh, Md. Mishkatul Islam, and Md. Mahmudul Hasan

Department of Electrical and Electronic Engineering, Bangladesh University of Engineering and Technology

Abstract: Array of sub-wavelength holes etched on to a thin metal film is a class of plasmonic structure, more commonly known as a metal nanohole array (NHA). This class of structure exhibits surface plasmon (SP) resonance. The SP resonance in metal NHAs are composite of the two main kind of plasmonic resonance - the surface plasmon polariton (SPP) resonance and localized surface plasmon resonance (LSPR) along with evanescent propagating waveguide modes. This variety and richness in the physics of their resonant characteristics, make metal NHAs attractive and useful in various field of application, from refractive index sensing to light emission and photovoltaics. When special configurations are made using metal NHAs, they also exhibit some special resonance, like Tamm plasmon (TP) resonance, Fano resonance, absorption induced transparency (AIT) and surafce lattice resonance (SLR). In this review, the physics and application of metal NHAs is presented. In presenting the physics of metal NHAs, the physics of single sub-wavelength holes and sub-wavelength hole arrays (NHAs) on metal films are described, by analysing their transmission and dispersion relation characteristics. Thereafter, some of the devices reported so far, whose operation are based on the optical characteristics of metal NHAs are presented. Application of mtak NHAs in the fields of biosensing, light emission - lasers, photo-voltaics, optical communication etc are presented and analysed. Finally, based on the current trend of research in this field, the future of metal NHAs is presented.

Keywords: Nanohole array | Plasmonics | Metamaterials | Nanophotonics

Table of Contents

1. Introduction

SS: Plasmonics as a field has seen a boom since the 2000s owing to the development of sophisticated fabrication technologies. In plasmonics, certain metals such as gold (Au), silver (Ag), aluminium (Al) are prerequisites. Plasmonics is attractive and relevant because they can confine light beyond the diffraction limit into sub-wavelength spaces, show intense local electric ($|\vec{E}|$) field concentration and sensitive narrowband emission [1]. Thin metallic sheets, metallic nanoparticles and metal films perforated with nanholes are the usual structures seen in plasmonic devices. Holes perforated on metallic films have special properties not seen in metallic nanoparticles or thin metal sheets. The subwavelength features of the nanohole edges along with the continuity of metallic film, makes metallic voids and metallic nanohole arrays exhibit a richer variety of plasmonic effects than other forms metallic nanostructures.

The prefix '**nano**' for the case of this review, primarily refers to sizes comparable to or smaller than a quarter of the wavelength of incident light. When aperture dimensions are much greater than incident electromagnetic (EM) wave wavelength classical electromagnetic theory and it's approximations are sufficient in explaining the physics of the associated wave transmission mechanism [2]. However, the novel physics for sub-wavelength **nanoholes** was reported for the first time in the seminal work of Ebbesen et al. in 1998. A square array of nanoholes on a gold film was reported to exhibit greater than unity transmission, when normalized to the fraction of hole area in a unit cell of the array [3]. The phenomenon of such an enhanced transmission via an array of nanoholes has been the topic of intense research. There has been numerous works

Author Declarations: The authors declare that no part of this report has been plagiarized, and all relevant sources are properly cited to the best of their knowledge. The individual contribution of each author is marked by the initials of the author at the beginning of each section/paragraph. Authors also agree that this manuscript is not to be submitted for publication without prior consultation and approval from the course instructor.
Disclaimer: This paper was written for the EEE 6505 - Nanophotonics and Plasmonics course of the Department of Electrical and Electronic Engineering, Bangladesh University of Engineering and Technology (BUET). The paper has not been peer reviewed, and should be treated as a term paper written by graduate students. The course instructor for the course is Dr. Sajid Muhaimin Choudhury, Department of EEE, BUET.
Student ID of the Authors: SS: 0421062311, RS: 0421062321, MMI: 0421062524, MMH: 0421062325
Correspondence: All correspondence regarding this paper is to be made to **Dr. Sajid Muhaimin Choudhury** sajid@eee.buet.ac.bd

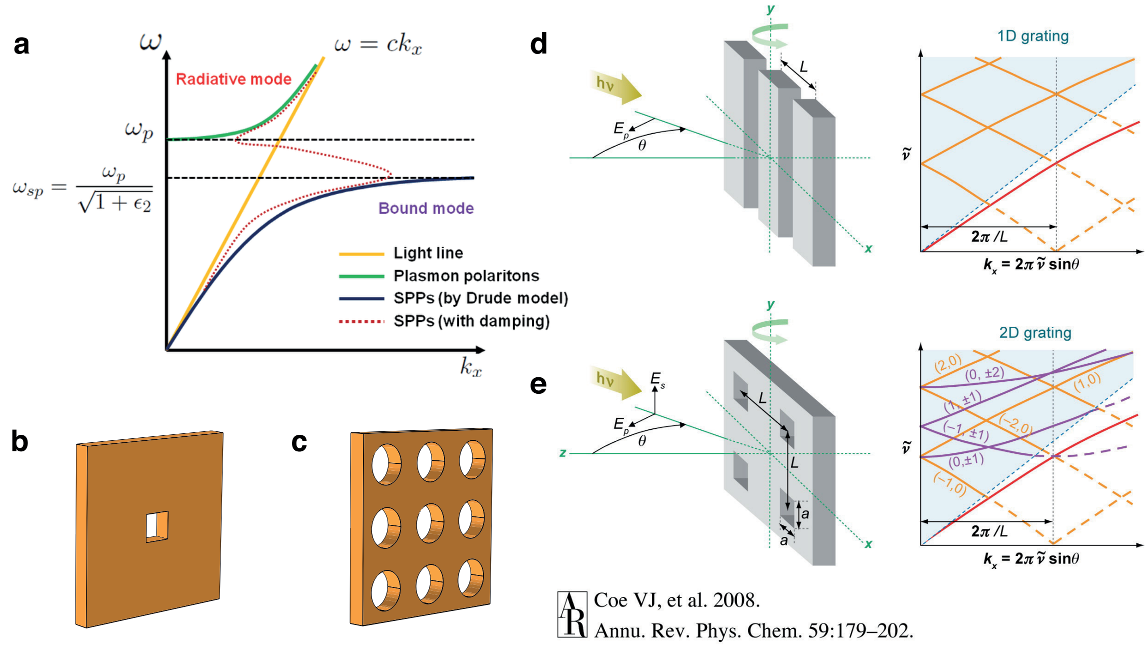

Fig. 1. a. Dispersion relation of SPPs on a continuous metal-dielectric, ω_p is the bulk plasma frequency and ω_{sp} is the surface plasmon frequency. **b,c.** Schematic of a metal with a single subwavelength square aperture **(b)** and a nanohole array (NHA) **(c)**. **d,e.** The infolding and repetition of the SPP dispersion on a metal surface patterned with a one dimensional grating and a two dimensional NHA. ν represents the reciprocal wavelength while k_x is the incident wavevector component along x-direction. Plot **(a.)** is obtained from Ref. [4]. Figure **d,e** are obtained from Ref. [5]

.

in explaining the origin and application scope of metal nanohole arrays (NHAs) over the years since 1998.

Till date, there has been many reviews on plasmonic devices, featuring holes and hole arrays [5–14]. However, most of these works focus on predominantly sensing application of metal NHAs or simply, the theoretical treatise of patterned metal NHAs. Our work focuses on a review across all fields covering, plasmonic sensing, light emission and lasing applications, photovoltaic applications and terahertz applications.

2. Nanoholes and their physics

SS: Classical electromagnetics predicts very weak transmittance through sub-wavelength hole(s) on thin ideal metallic films, where the effects of surface plasmons were ignored. Electromagnetic waves passing through holes perforated into a perfectly conducting and infinitely thin film suffer from diffraction. However, diffraction effects are minimal for hole sizes much greater than the wavelength of incident light. Much of the theory of diffraction from a hole on an infinitely thin, perfectly conducting screen can be obtained from the treatise of Bouwkamp [15]. Transmission through an aperture of radius $\boldsymbol{r}$ much greater than the wavelength ($\boldsymbol{\lambda_0}$) of incident wave could be described by the following set of equations, where diffracted fields is much less than transmitted fields.

$$I(\theta) \cong I_0 \frac{k^2 r^2}{4\pi} \left| \frac{2J_1(krsin\theta)}{krsin\theta} \right|^2 \qquad [1a]$$

$$T = \frac{\int I(\theta) d\Omega}{I_0} \qquad [1b]$$

Here, $\boldsymbol{k = 2\pi/\lambda_0}$ is the wavenumber, $\boldsymbol{\theta}$ is the angle between the normal to the aperture surface and the direction of diffracted wave and $\boldsymbol{J_1}$ is the first order Bessel function. The transmitted intensity is normalized to the incident intensity of $\boldsymbol{I_0}$ on a hole of area $\boldsymbol{\pi r^2}$ to obtain the normalized transmitted coeffecient, $\boldsymbol{T}$. $\boldsymbol{T \approx 1}$ for $\boldsymbol{r \gg \lambda_0}$.

A. Single nanohole. The primary conclusion from the preceding discussion is that the presence of the conducting film, made no difference to the transmission of waves through the area of the holes. Thus the incident wave does not interact with the opaque screen. While this assumption holds approximately true for $\boldsymbol{r \gg \lambda_0}$, it fails as $\boldsymbol{r}$ approaches wavelength dimensions; diffraction effects become all the more prominent in comparison to the physics of the un-diffracted, transmitted beam. Bethe gave an exact analytical relation between $\boldsymbol{T}$ and $\boldsymbol{r}$ for a single sub-wavelength aperture on an infinitely-thin opaque screen; the relation can be described by the following equation, which is limited up to the 4th power term [16]. Bouwkamp included higher order terms in the equation in his treatise [15].

$$\begin{aligned} T &= \frac{64}{27\pi^2}(kr)^4 \\ &\propto (\frac{r}{\lambda_0})^4 \end{aligned} \qquad [2]$$

Thus, the transmission through a single sub-wavelength nanoaperture is rather weak and scales inversely to the power of 4 for wavelengths greater than the hole radius. Further including the effects of finite thickness of the perfectly conducting film, shows an exponential decay of transmitted beam with film thickness, indicating the tunnelling of waves through conducting film with apertures [17]. Further incorporating the effects of a real metal as opposed to a perfectly conducting film further dictates that optically thin films are not perfectly opaque. And films which are several skin depths thick do not support tunnelling.

If the metallic character and infinite thinness are not approximated, the role of plasmons become all the more important in explaining the physics of transmission through a single nanohole on a metal film. This gives greater convergence with experimental results. Classical diffraction theory is not sufficient in explaining transmission through subwavelength apertures. In this regard, the role of surface plasmons – both propagating and localized – were explored in greater depth since the work of Ebbesen et al. in 1998 [3].

Light impinging on a single sub-wavelength aperture, excites propagating SPs, known as surface plasmon polaritons (SPPs) [18–20]. SPPs are primarily responsible for enhanced transmission through sub-wavelength apertures. Also, at the edges of the nano-aperture, the surface plasmons are localized, leading to the formation of localized surface plasmon resonance (LSPR). The LSPR can tunnel through to the transmission side of the metal film via the aperture [21]. However, the transmission is still relatively weak and further enhancement was achieved through an array arrangement of nanoholes.

B. Nanohole array. The role of SPPs and coupling of LSPRs become prominent in metal NHAs, than that in single nano-apertures. The weak transmission due to that of sub-wavelength holes in metals because of being diffraction limited, can be overcome by arranging the holes in a periodic array. In such a case the NHA shows unusually high transmission, even for longer wavelengths, in clear violation of Bethe's analytic relation given in Eqn. 2 [3]. In a broad strokes, it can be said that the reason for this high transmission is attributable to surface plasmon resonance on the metal interface.

The contribution of SP resonance in enhnaced transmission of certain wavelengths can be classified into three physical phenomena.

- **Surface Plasmon Polariton (SPP):** Plasmons propagating on the metal surface are the prime contributors in the extraordinary transmission through a metal NHA [22, 23]. The in-folding of the SPP dispersion relation at integer multiple positions of the reciprocal lattice period in the k-domain, results in modes within the light line that can be coupled to radiative modes [5, 24]. This can be seen in the dispersion relation of SPP waves on a metal NHAs, as seen in **Fig. X**. The dispersion relation in Fig. 1 is dictated by the following equations.

$$\begin{aligned}\vec{k}_{spp} &= \vec{k}_x \pm i\vec{G}_x \pm j\vec{G}_y \\ &= \frac{\omega}{c}\sqrt{\frac{\epsilon_d \epsilon_m}{\epsilon_d + \epsilon_m}}\end{aligned} \quad [3]$$

  Here, $|\vec{G}_x| = |\vec{G}_y| = 2\pi/a_0$ are reciprocal lattice vectors along x- and y-directions, where a_0 is the period of the holes in the nanohole array. The permittivity of dielectric and metal are denoted by $\epsilon_{d,m}$. The $\vec{k}_{spp}$ is the SPP wavevector and $\vec{k}_x$ is the component of incident wavevector along x-direction. The order of modes are indicated by i, j. Solving Eqn. 3 for normal incidence, the following analytic relation is obtained.

$$\lambda_{spp}(i,j) = \frac{a_0}{\sqrt{i^2 + j^2}}\sqrt{\frac{\epsilon_d \epsilon_m}{\epsilon_d + \epsilon_m}} \quad [4]$$

  In this relation, $\lambda_{spp}(i,j)$ indicates the (i,j) order SPP modes excited via normal incidence.

- **Localized Surface Plasmon Resonance(LSPR):** Metallic nanoparticles excite localized surface plasmon resonance (LSPR), whose resonances are broader than SPPs due to damping but are effectively confined to sub-wavelength spaces as well [1, 25]. In the case of nanohole arrays, the field permeates into the metal film exciting LSPs at the hole edges and ridges. If both interfaces of the metal film have the same dielectric, then the energies of LSP modes at both ends are same, and significant tunneling through the holes occur via LSPR [21]. Compared to SPP resonance, LSPR effects in metal NHAs is weak [24]

- **Waveguide modes:** Holes perforated on to metal films act as nanoscale waveguides for electromagnetic (EM) propagation.

An opaque metal film, excites SPs propagating along the metal dielectric interface, known as surface plasmon polariton (SPP). SPPs show highly coherent resonance and are highly localized at the metal-dielectric interface. There is little transmission of EM radiation through the film, as the perpendicular decay of the surface plasmon is well below the diffraction limit. however since On the other hand

Metal NHAs on the other hand exhibit a bit of both SPP and LSPR resonance. Perforating an opaque metal film with sub-wavelength holes will not only open a channel for wave transmissions, but also show amplification of the transmitted wave.

SPP resonance shows a characteristic E-k curve as shown in Fig. 1. When patterned along one axis only, the E-k diagram the SPP dispersion repeats periodically along the k axis. This causes an overlap in the Energy modes of the structure. Similarly, having a two-dimensional array on the metal surface causes similar effects along both the kx and ky directions. This results in an overlap of energies in the Brillouin zone, which opens up the possibility of normal excitation (k=0), that is not possible with SPPs on a flat metal slab on dielectric.

C. Effect of hole shapes:. The effect of nanohole shapes have been studied theoretically by Koerkamp et al. [26]. Changing shape of the nanohole from a circle to rectangle increases the transmission, whilst also causing red-shift in resonance wavelength. The effect of shape in resonance, termed as shape resonance, is a strong component of LSPR along the hole edges. Despite a reduction in overall hole area, the transmission increases. In this regard, the aspect ratio of the two hole dimensions in a rectangular hole, affect the spectral position of transmission modes [27].

D. Factors affecting transmission through nanoholes:.

E. Special plasmonic modes:. When incorporated with other structures, some specialized surface or bulk plasmon modes exists such as fano-resonance, Tamm plasmon resonance or Surface lattice resonances exist. Contarry to a single nanohole on a metal film, an array of nanoholes can effectively act as a metamaterial.

E.1. Tamm plasmonic resonance:. When a smooth plasmonic metal film is placed on top of a distributed Bragg reflector (DBR), specialized surface states are formed at the metal-DBR interface due to the abrupt end of the periodic index variation of the DBR. These states are called Tamm plasmon (TP) or optical Tamm states (OTS) keeping in similarity with the analogous surface states of electronic crystals, which were named after the discoverer scientist Igor Tamm [33]. Propagating TP states at a metal-DBR interface were

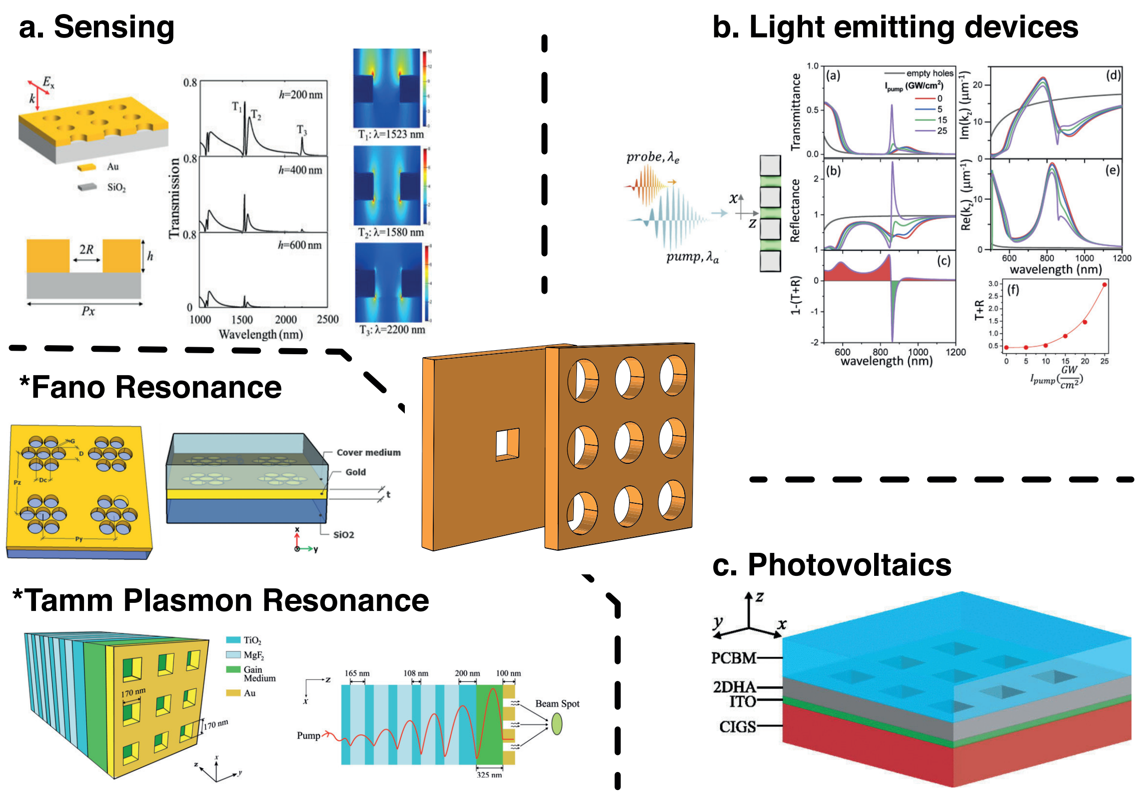

Fig. 2. The potential application scopes for metal nanohole arrays along with the special plasmonic modes. The structures depicted in reference to Fano Resonance and Tamm Plasmon resonance have been sourced from Ref. [28] and Ref. [29]). Metal NHAs are popularly used in **a.** Sensing [30], **b.** light emission related applications [31], such as lasers and in **c.** photovoltaics [32].

first theorized in 2007 and experimentally reported a year later [34, 35]. These (Tamm) plasmonic states suffer from less loss and can be excited by normal incidence. They can also be coupled to radiative modes without any sort of additional structural additions. This makes Tamm plasmonic structures good candidates for lasing applications.

Confined TP states observed for a continuous metal film on top of DBR, can be tuned by patterning the metal film. Using micrometer-scale disk array patterns [36], rectangular patch patterning [37], or one-dimensional (1D) array of thin metallic strips [38, 39] results in tailoring the dispersion relation of Tamm plasmons. In this regard, etching a single nanohole on the metal film of a Tamm plasmon structure or put differently, adding a DBR on top of single nanohole in a Au film, results in enhanced transmission through the hole [40, 41].

E.2. Fano resonance. Fano resonance shows a non-lorentzian asymmetric spectral mode lineshape. It occurs due to the combination of discrete states and states in continuum. This has made Fano-resonant structures ultra sensitive and appropriate as plasmonic detectors and sensors [42]. Hajebifard et al. reported fano resonance due to the interference of transmitted waves with LSP/SPP waves and Wood's anomaly waves [43] in gold heptamer nanohole arrays [28]. Their structure exhibited high bulk and surface sensitivity for fano resonance due to LSP waves and high figure of merit for the fano resonance due to SPP and Wood's anomaly modes. These reports on the use of metal nanoholes to generate fano resonances, can be utilized in sensing applications.

E.3. Absorption Induced Transparency (AIT). NHAs are prime candidates for absorption induced transparency (AIT). AIT occurs for certain types of absorbent molecules placed adjacent to the metal nanohole array. It is a non-intuitive phenomenon of transmitting radiation that falls within the absorption band of the molecular excitation proximal to metal nanohole array. This unique phenomenon can explain the anomalous transmission peaks when absorbent molecules are placed adjacent (or on top) of metal nanohole arrays. The emission in this regard is definitely contributed by the surface plasmon excitation, but is not dependent on the periodicity or hole dimensions of the NHA [31, 44].

3. Application of NHAs

As seen from the preceeding discussion, extraordinary transmission from metal NHA has contributions from SPP, LSP and propagating waveguide modes. This has led to a richness and variety in it's application spectrum. The field enhancement around the nanohole edges is optimal for photovoltaic applications.

Among the different classes of plasmonic structures available, metal nanohole arrays are particularly useful for sensing, lasing, absorption, and photovoltaic purposes. Metal nanohole arrays in this regard show unusual properties, because of its plasmonic effects. EOT has opened up a new perspective in transmission through nanohole arrays [45].

A. Sensing and imaging. MMH: In previous review papers on the plasmonic based biosensor on viral diagnosis have covered the colorimetric method, Raman scattering, propagating surface plasmon resonance (SPR), localized SPR and fluorescence [46, 47]. One of them has also shown the progress of viral detection using plasmonic bio sensors and discuss about the application of this method for covid-19 detection [47]. But in this paper, the main focus will be on metallic plasmonic nanohole based viral detection and how they improve the sensitivity of the sensors.

Biosensors are one of the major application field for plasmonic nano-hole arrays. During the corona pandemic period this application seems more useful for rapid viral detection. Rapid viral detection is one of the main parts of stopping spreading of the virus. Some previous work on various virus detection has been done using Optofluidic Nano plasmonic Biosensor and Optical Trapping by nano plasmonic biosensors [58,59]. The Optofluidic Nano plasmonic Biosensor have given a proof-of concept biosensing stage for quick, compact, quantitative, and label-free detecting of viral particles with minimal sample processing [48]. The process of detecting the virus utilizing the extraordinary light transmission phenomena, highly tunable frequency and refractive index sensitivity (RIS) on plasmonic nanohole arrays is quite convincing [49]. This method uses antiviral immunoglobulins immobilized on the surface of the nanohole arrays which shown that it's capable to detect various types of virus directly [58]. The most important part of this method is it can be done directly utilizing the typical biology laboratory settings. Which is quite crucial during pandemic time because shortage of resources.

The optical trap in nanohole arrays is another method to detect viruses using plasmonic nanohole array-based bio sensors. This method uses classical electromagnetic theory and light-driven operation [50, 51]. In this method the virus is guided by the electromagnetic wave (light) to trap that in the nanohole arrays which eventually changes the spectral peak. This resonance shift and potential energy of the trapping systems put an effect on the local field intensity of electromagnetic wave [50]. Eventually this method has been shown high sensitivity towards detecting the virus. Though there are some other methods to enhance the sensitivity of the nanohole array for a label-free viral detection is using an extra sensitive Ag-Au alloy nanohole arrays. This Alloy nanostructures disclose the unique plasmonic phenomena that supersede the pure metallic options [52]. Another unique method called "Double-Langmuir Model" can be used for plasmonic nanohole array-based bio sensors for viral detection [53]. Considering all these methods each has special application depending on resource and environment. But if it is considered for the pandemic period then the plasm fluidic biosensor based viral detection is the best solution. It is fast, reliable, require minimal resources and requires zero additional laboratory setup.

A.1. Biosensor related applications. RS: Plasmonic nanohole arrays have a multitude of applications in the field of biosensors.Two such applications are discussed below.

Real time analysis of live cell secretion. RS: In order to understand physiological and pathological processes,it is vital to investigate cellular functions.Proper understanding of the above mentioned processes will help with the improvement of diagnosis.[54] In Xiokang et al.,an integrated biosensor consisting of two complementary and adjustable microfluidic modules, namely the cell culture module and the optical detection module was developed(Figure-3(a)). For the microfluidic cell module, they fabricated a single zigzag channel in a polydimethylsiloxane (PDMS) slab that was permanently bonded to a glass slide (Figure-3(b)).[54] The cell module consisted of inlet and outlet tubing connections and the growth area could be adjusted to increase or decrease the number of cells produced.The nanoholes (200 nm diameter, 600 nm period) were fabricated by deepUV lithography on freestanding SiNx membranes, and each NHA was defined to have an area of 100×100 μm (Figure-3(c)).[54].There were three parallel microchannels in the microfluidic system.[54]. Before measurement,the sensors were characterized for VEGF detection by using well-known biotin/streptavidin interaction for the biofunctionalization of the NHA sensors (Figure-3(d)). The EOT spectrum shown in Figure 3e relates the shift in wavelength to the number of antibody bonding taking place in the sensor and hence enabling measurement.

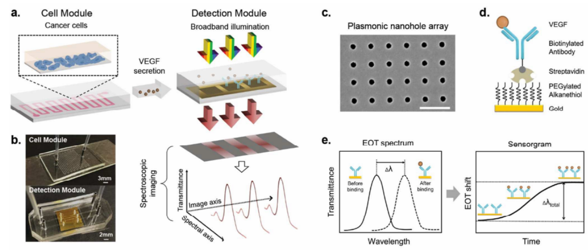

Fig. 3. (a)The biosensor system consists of the microfluidic cell module and optical detection module. Cancer cells grow in a zigzag single-channel PDMS unit, and the secreted cytokines are directly delivered to the adjacent detection module.(b) Cell culture module bonded to a gelatin-coated glass slide with inlet and outlet connections (top), and the detection module consisting of the plasmonic chip embedded in a microfluidic system with three independent channels (bottom). (c)SEM image of the nanohole structures with a hole diameter of 200 nm and a periodicity of 600 nm. Scale bar: 1 μm. (d)The illustration shows the surface chemistry utilized for specific VEGF detection, where the antibody is immobilized by the robust streptavidinbiotin interaction. Streptavidin is covalently bonded to the activated carboxylic groups on the PEGylated alkanethiol molecules sitting on the gold surface.(e)Sensing principle of the real-time plasmonic detection. The EOT spectrum from each nanohole array shows a characteristic resonance peak (solid line). Biomolecular binding on the sensor surface induces an EOT spectral shift of the peak (dashed line). As molecular binding accumulates, the spectral displacements of the resonance peak are then plotted in the sensorgram (EOT shift vs. time) to reveal the real-time binding dynamics.[54]

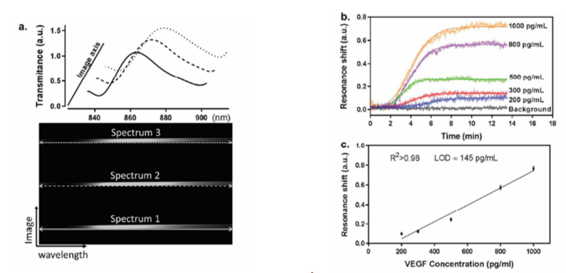

Fig. 4. (a)The spectral image recorded by the spectrometer and CCD camera shows the spectral information from the three in-line NHA sensors simultaneously (bottom). Each spectrum is then extracted from the image, showing the EOT resonance peaks for detection analysis (top).(b) The sensorgrams of the direct detection of VEGF ranging from 200-1000 pg/mL. (c)Standard calibration curve for VEGF detection. Data plots represent the mean and standard deviation of each concentration measured in triplicate. Plots are fitted to a linear regression model (R2 > 0.98), and the Limit of Detection (LOD) is calculated as the concentration corresponding to 3 times the standard deviation of the blank signal. [54]

In Xiaokang et.al,optimal condition for VEGF secretion from HeLa cells was probed.The stimulation scheme for VEGF secretion in HeLa cells was determined.At first,the endogenous production of VEGF was confirmed by immunofluorescence assay(Figure-5(a)).[54]. Calcium ionophore named A23187 was used to stimulate VEGF secretion as it can increase the intracellular Calcium ion levels rapidly allowing divalent ions to cross plasma membranes.Cells were grown in multi-well plates and incubated overnight with different concentrations of A23187, ranging from 1 to 100 μM. Supernatants were collected and analyzed by sandwiched VEGF ELISA assay.. As shown in Figure 5b, the VEGF secretion showed a biphasic profile depending on the concentrations of A23187. A marked increase in VEGF production was achieved with 1 and 10 μM of A23187, which was more than two times higher than the control group(i.e. without stimulus).[54]

The impact of different serum concentrations was also observed.VEGF secretions from HeLa cells were observed under 1%,5% and 10% concentrations of serum.Even though serum free media and 1% serum media displayed reduced secretion compared to 10% serum media due to cell death during incubation,5% serum media maintained significant secretion(Figure-5(b) and (c)).[54]

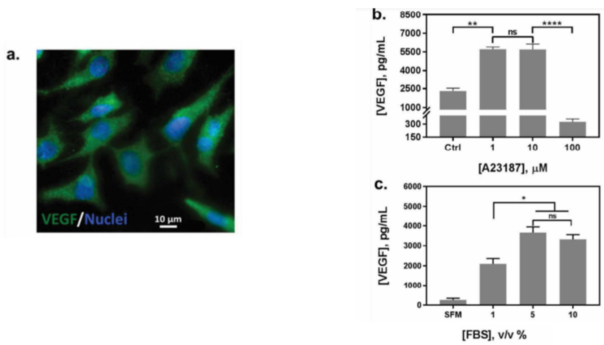

Fig. 5. (a)Immunofluorescence assay for the confirmation of endogenous production of VEGF in HeLa cells. VEGF was stained with AlexFluor 488 (green) while cell nuclei were highlighted by DAPI (blue).(b) VEGF concentration measured in cell culture supernatants after administration of calcium ionophore at different levels. (c)VEGF concentration measured in cell culture supernatants in presence of different serum concentrations ([FBS] = 0 as SFM; p<0.05: *; ns: non-significant; n=2).[54]

Nanohole arrays for Surface Plasmon Resonance biosensing. RS: In Hyungsoon et al.,template stripped smooth Ag nanohole arrays with Silica shells were analyzed for application in Surface Plasmon Resonance based Biosensing.Template strip technique leverages mature silicon processing technology to make a precisely patterned Si master template.[55].The pattern is then transferred to a deposited metal film, which can be peeled off on demand using an adhesive backing layer.[55].This produces smooth patterned surfaces essential for Plasmonic Biosensing.Electromagnetic fields of Surface Plasmomic waves are limited to 10-100nm of the metallic surface.[55].So slight roughness in the surface can result in poor performance of the sensor. The fabrication process of template stripped Ag nanohole arrays is shown in Figure 6.The process combines template-stripping with atomic layer deposition (ALD) to produce periodic nanohole arrays in smooth and optically thick (>100 nm) Ag films, which are subsequently encapsulated with an ALDgrown silica shell for real-time SPR biosensing.[55]. . Nanoimprint lithography is used to pattern the reusable Si master templates, from which Ag nanohole arrays are replicated with metal deposition and a one-step, peel-off process using optical epoxy as a backing layer.[55]. Figure 7 demonstrates the optical characteristics of Template Stripped Ag nanohole array.Those are measured experimentally for a nanohole array with 180nm hole size and 500nm hole separation.The optical transmission spectra of tem-

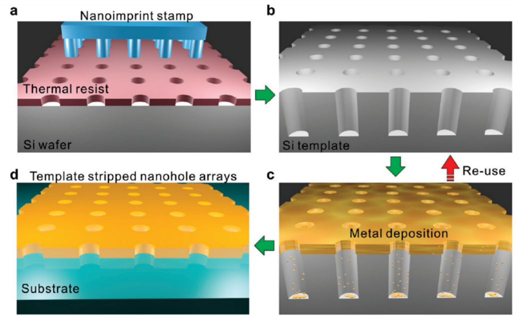

Fig. 6. (a) Thermal resist layer spun on a Si wafer is imprinted with a nanoimprint stamp with circular post patterns.(b) Si wafer is subsequently etched to be a nanohole template with deep circular trenches.(c) Metal film is directionally deposited on the Si template.(d) Metal surface is coated with a thin layer of epoxy and covered with a glass slide. The Ag film is then peeled off of the template to reveal the smooth nanohole array made in the metal film. The Si template can be reused to make multiple identical samples.[55]

platestripped Ag nanohole arrays were measured with illumination by a tungsten halogen lamp through a microscope objective (5, NA = 0.15) and collected with a fiber-optic spectrometer.[55]. The optical transmission characteristics of nanohole arrays in contact with medium with different refractive indices are displayed in Figure 7a.Figure 7b indicates the correlation between refractive index and spectral shift.It can be concluded that increasing refractive index of medium can result in higher spectral shit in the transmission characteristic.This feature can potentially be used to detect organic substances.

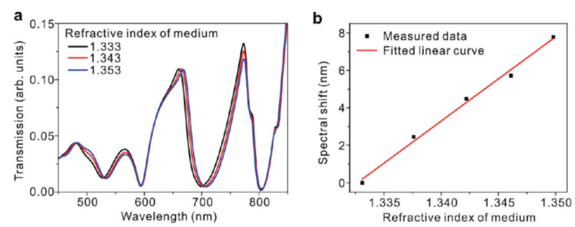

Fig. 7. (a) Experimentally measured optical transmission spectra through the nanohole arrays with 180 nm hole size and 500 nm periodicity made in a 100 nm thick Ag film. The bulk refractive index of a water ethanol mixture on the Ag film varies from 1.333 to 1.350.(b) Bulk refractive index sensitivity measurements of the fabricated nanohole arrays shown in panel a. The spectral shifts are measured as the refractive index of the waterethanol mixture changes from 1.333 to 1.350. The calculated bulk sensitivity is 450 nm/RIU (RIU = refractive index unit). The solid red line shows a fitted linear curve.[55]

B. Light related application. A lot of nanoscale light emitting and absorbing devices employ plasmonics to enable the extreme confinement of light. Metal NHAs have better transmission capability to transmit light than nanoparticle arrays. The field enhancement at the hole edges of nanohole arrays cause high absorption as well. These features make metal NHAs attractive in light related applications

Due to the development of sophisticated fabrication and lithography techniques, such as ion beam milling, nanoimprint lithography has contributed to the ease of experimentation of metal NHAs as electrodes in light emitting devices and photovoltaic applications; in constructing resonant cavities for plasmonic lasers and as nanoantennas for terahertz (THz) wave generation. In this regard the anomalous phenomenon of absorption induced transparency (AIT) can be utilized as well. This section discusses the application of metal NHAs in all such plasmonic devices operating in the visible range.

B.1. In light emitting diodes. Light extraction efficiency in an organic light emitting diode (OLED) can be increased by patterning metal electrodes by replacing opaque metal with metal nanohole arrays [56, 57]. Apart from this, the main advantage of plasmonics in the case of light emission sources lies in confining light beyond diffraction limit.

B.2. Lasers. Ohmic losses in plasmonic materials is a problem. A way to copmpensate these losses in plasmonic light sources is done by using gain materials [58–60]. Plasmonic lasing intermediated by metal nanohole arrays was first reported experimentally by Beijnum et. al. [61]. The lasing emission in this demonstration was attributed to the surface plasmon mode of the structure, as confirmed by their wavelength- and angle-resolved analysis. This demonstration of plasmonic laser was considered advantageous because: firstly, the dispersion relation calculation could be calculated from the far field data; the shape of the laser beam can be analyzed due to its compactness and lastly, the resonator can be studied by the help of a simple mathematical simple model.

B.3. Photovoltaics. For efficient conversion of solar energy into conduction electrons, broadband absorption spectrum is needed in photovoltaic structures. While thicker layers can increase absorption, they reduce the minority carrier diffusion length, hence reducing current flow. Layers of materials with increasing band gap are placed in tandem. Lattice matching and photocurrent matching are important considerations for combining two or more photo-absorbent layers which limits the choice of materials that can be used. In this regard, using an intermediate plasmonic NHA bypasses these constraints besides increasing the short circuit current density. Compared to metallic strips and mtallic nano clusters, metallic NHAs give greater increase in short circuit current density. Besides, metallic NHAs are excellent scattering agents, that increase the photon path length, slowing down light within the cells. The use of transparent conducting electrodes (TCEs) is ubiquitous in optoelectronics. They are electrically conductive optically transparent material. Besides having use in touchscreen displays such as in organic light emitting diodes (OLEDs), active-matrix OLED (AMOLED), thin film solar cells, e-papers, flexible displays etc [62]. Despite high consumer demand, the availability of such materials is rare. Indium Tin Oxide (ITO) is the currently the most popular choice, for TCEs offering over 90 % transmittance of the visible spectrum and a low sheet resistance upto 10 Ω. It is widely used in thin film polymer solar cells. However, ITO has a high cost, is structurally very brittle and has a highly thickness dependent conductivity. Metal NHAs have been touted as a possible replacement for ITO [63]. In thin film photovoltaics, plasmonics can essentially reduce the layer thickness and increase absorption by increasing scattering, light confinement and creating hotspots [64].

Metal NHA based thin film solar cells were first demonstrated by [65]. Kishwar et al. later reported around 12 % increase of short-circuit current density compared to a cell without any intermediate plasmonic layer [32, 66]. This increase in short-circuit current density is almost thrice more than that reported for an array of metal nanoparticles.

C. THz Band applications. MMI: In 1998 Ebbesen et al. reported intriguing measurements of the optical transmission through thin-film metal gratings[3]. It was later demonstrated that the optical transmission through subwavelength holes in metal films can be enhanced by several orders of magnitude[67]. In 2003 Rivas et al. presented measurements of the transmission of terahertz radiation through periodic arrays of holes (70*70 μm) made in highly doped silicon wafers. Sharp resonances and enhanced transmissions were observed .This anomalous transmission is attributed to the resonant tunneling of surface-plasmons polaritons. As Gratings are structured in doped silicon and for the metallic behavior of doped semiconductors at THz frequencies, it was demonstrated that it was possible to excite surface plasmon polaritons on these structures and to tunnel them through subwavelength holes. This observation paves the way for using subwavelength apertures for the development of sensitive THz imaging systems [68].Ali Forouzmand et al. demonstrate that a wire medium slab loaded with graphene nanopatch metasurfaces (GNMs) which enables the enhancement of evanescent waves for the subwavelength imaging at terahertz (THz) frequencies. The dual nature (capacitive/inductive) of the GNM is utilized in order to design a dual-band lens in which the unique controllable properties of graphene and the structural parameters of wire medium (WM) slab provide more degrees of freedom in controlling two operating frequency bands. The lens can support the subwavelength imaging simultaneously at two tunable distinct frequencies[69].

Miyamaru et al. proposed a surface-wave sensor based on the resonant transmission characteristics of metal hole arrays which is demonstrated in the terahertz (THz) region. A layer of substance (thickness lees than 5 μm) much thinner than the wavelength of the THz wave (THz=1 mm at 0.3 THz) is attached to the surface of a metal hole array(500 m thick metal slab perforated with an array of circular holes distributed along a triangular grid , with holes of diameter of 680 μm, and the lattice constant of the triangular array is 1130 μm) and it was demonstrated that the existence of such a small amount of substance can be detected more easily than without the metal hole array. This demonstration of THz sensing with metal hole arrays indicates the possibility of realizing THz surface-wave sensors for biochemical molecules in the THz region[70].

The transmission response of metallo-dielectric grid metasurfaces is experimentally investigated through Terahertz Time Domain Spectroscopy for investigating the family of SPP excitations observable below and above the transition frequencythat separates the plasmonic/metamaterial region from the photonic crystal regime. Further work can be done in this area by nanoscale grid metasurfaces using suitable metallic patch for sensing and subwavelength imaging In THZ frequencies [71].

A photonic switch is an integral part of optical telecommunication systems A plasmonic bandpass filter integrated with materials exhibiting phase transition can be used as a thermally reconfigurable optical switch which offers an attractive platform to bridge the size mismatch between optical devices and electronics and hence enable compact integration of these devices on a single chip.Aluminium NHAs on quartz was used in plasmonic switch using the semiconductor-to-metal phase transition of vanadium dioxide. The fabricated switch shows an operating range over 650 nm around the optical communication C, L, and U band [72].Terahertz-band (defined as 0.1 to 10 THz - wavelengths of 3 mm to 30μm) communication has been envisioned as a key wireless technology to satisfy the need for much higher wireless data rates[73][74].A promising approach to realizing THz communications is to leverage the properties of plasmonic materials mainly graphene which supports the propagation of THz surface plasmon polariton (SPP)(

In conventional plasmonic materials, SPPs propagate only in the infra-red and above) waves and has excellent electrical conductivity, making it very well suited for propagating extremely-high-frequency electrical signals[75][76].In this paper, it was analytically and numerically investigated the temporal dynamics of graphene-enhanced metallic grating structures(a 300 nm-thick grating, with a 200 nm duty cycle,the range of the grating period was from 300 to 1600 nm) used for excitation and detection of SPP waves at THz frequencies.The results further motivate the use of grating-gated graphene-based heterostructures as tunable SPP wave sources, modulators and detectors[77].

4. Future prospects

SS: The relevance and increasing use of plasmonics in different fields of application has made metal nanohole arrays an apt choice as resonant structures. This review explains and discusses the potential of metal nanohole arrays in different scopes. The use of nanohole arrays in novel and interesting physics which will only be explored further in the future is important too.

Plasmonic bio-sensors based on the resonance of plasmonic nanohole arrays exhibit huge potential in areas of sensing, especially in case of virus detection [46]. Nanohole arrays in this regard are especially useful, among other classes of plasmonic sensors, since they have been well integrated with flow based sensing systems [78–80]. The phenomenon of AIT and fano resonances are likely to dictate the future direction of research and application of metal nanohole arrays in light related applications [4, 31, 44]. These effects will have immense potential for next generation solar cells and light emitting devices. Perfect electrical conductors with holes in them are considered to be novel plasmonic metamaterials [81]. Recently, freestanding metal nano-membranes with nanohole arrays have been fabricated for ultra-sensitive wavelength filtering. Plasmonic materials are gradually shifting towards nitride-metal composites. The sensing and light concentrating capability of these novel materials will likely dictate the future direction of research in plasmonic nanohole arrays [82].

5. References

1 SA Maier, *Plasmonics: Fundamentals and Applications.* (2007).
2 JD Jackson, *Classical Electrodynamics.* (John Wiley & Sons, Inc.), (1998).
3 TW Ebbesen, HJ Lezec, HF Ghaemi, T Thio, PA Wolff, Extraordinary optical transmission through sub-wavelength hole arrays. *Nature* **391**, 667–669 (1998).
4 S Kaya, Ph.D. thesis (2016).
5 JV Coe, JM Heer, S Teeters-Kennedy, H Tian, KR Rodriguez, Extraordinary Transmission of Metal Films with Arrays of Subwavelength Holes. *Annu. Rev. Phys. Chem.* **59**, 179–202 (2008).
6 C Genet, TW Ebbesen, Light in tiny holes. *Nature* **445**, 39–46 (2007).
7 FJ Garcia-Vidal, L Martin-Moreno, TW Ebbesen, L Kuipers, Light passing through subwavelength apertures. *Rev. Mod. Phys.* **82**, 729–787 (2010).
8 Z Xie, et al., Plasmonic Nanolithography: A Review. *Plasmonics* **6**, 565 (2011).
9 AP Blanchard-Dionne, M Meunier, Sensing with periodic nanohole arrays. *Adv. Opt. Photonics* **9**, 891 (2017).
10 Y Luo, X Jiang, L Liu, G Si, Recent Advances in Plasmonic Nanolithography. *Nanosci. Nanotechnol. Lett.* **10**, 1–12 (2018).
11 K Yang, X Yao, B Liu, B Ren, Metallic Plasmonic Array Structures: Principles, Fabrications, Properties, and Applications. *Adv. Mater.* **n/a**, 2007988 (2021).
12 RG Parkhomenko, AS Kuchyanov, M Knez, MI Stockman, Lasing Spaser in Photonic Crystals. *ACS Omega* **6**, 4417–4422 (2021).
13 B Wang, et al., High-Q Plasmonic Resonances: Fundamentals and Applications. *Adv. Opt. Mater.* **9**, 2001520 (2021).
14 AD Utyushev, VI Zakomirnyi, IL Rasskazov, Collective lattice resonances: Plasmonics and beyond. *Rev. Phys.* **6**, 100051 (2021).
15 CJ Bouwkamp, Diffraction Theory. *Reports on Prog. Phys.* **17**, 35 (1954).
16 HA Bethe, Theory of Diffraction by Small Holes. *Phys. Rev.* **66**, 163–182 (1944).
17 A Roberts, Electromagnetic theory of diffraction by a circular aperture in a thick, perfectly conducting screen. *J. Opt. Soc. Am. A* **4**, 1970 (1987).
18 T Thio, KM Pellerin, RA Linke, HJ Lezec, TW Ebbesen, Enhanced light transmission through a single subwavelength aperture. *Opt. Lett.* **26**, 1972 (2001).
19 T Thio, et al., Giant optical transmission of sub-wavelength apertures: physics and applications. *Nanotechnology* **13**, 429 (2002).
20 AL Baudrion, et al., Coupling efficiency of light to surface plasmon polariton for single subwavelength holes in a gold film. *Opt. Express* **16**, 3420 (2008).
21 A Degiron, H Lezec, N Yamamoto, T Ebbesen, Optical transmission properties of a single subwavelength aperture in a real metal. *Opt. Commun.* **239**, 61–66 (2004).
22 L Martín-Moreno, et al., Theory of Extraordinary Optical Transmission through Subwavelength Hole Arrays. *Phys. Rev. Lett.* **86**, 1114–1117 (2001).
23 H Liu, P Lalanne, Microscopic theory of the extraordinary optical transmission. *Nature* **452**, 728–731 (2008).
24 FJG de Abajo, JJ Sáenz, I Campillo, JS Dolado, Site and lattice resonances in metallic hole arrays. *Opt. Express* **14**, 7–18 (2006).
25 , *Surface Modes in Small Particles.* (John Wiley & Sons, Ltd), pp. 325–380 (1998).
26 KJK Koerkamp, S Enoch, FB Segerink, NFv Hulst, L Kuipers, Strong Influence of Hole Shape on Extraordinary Transmission through Periodic Arrays of Subwavelength Holes. *Phys. Rev. Lett.* **92**, 183901 (2004).
27 KLvd Molen, et al., Role of shape and localized resonances in extraordinary transmission through periodic arrays of subwavelength holes: Experiment and theory. *Phys. Rev. B* **72**, 045421 (2005).
28 A Hajebifard, P Berini, Fano resonances in plasmonic heptamer nano-hole arrays. *Opt. Express* **25**, 18566 (2017).
29 Z Azad, MS Islam, MA Talukder, Mode-resolved analysis of a planar multi-layer plasmonic nanolaser. *Opt. Commun.* **482**, 126614 (2021).
30 AE Cetin, et al., Plasmonic Nanohole Arrays on a Robust Hybrid Substrate for Highly Sensitive Label-Free Biosensing. *ACS Photonics* **2**, 1167–1174 (2015).
31 SG Rodrigo, Amplification of stimulated light emission in arrays of nanoholes by plasmonic absorption-induced transparency. *Opt. Express* **29**, 30715 (2021).
32 K Mashooq, MA Talukder, Effects of intermediate plasmonic structures on the performance of ultra-thin-film tandem solar cells in *Physics, Simulation, and Photonic Engineering of Photovoltaic Devices VI.* (SPIE) Vol. 10099, pp. 120–125 (2017).
33 I Tamm, Über eine mögliche art der elektronenbindung an kristalloberflächen. *Zeitschrift für Physik* **76**, 849–850 (1932).
34 M Kaliteevski, et al., Tamm plasmon-polaritons: Possible electromagnetic states at the interface of a metal and a dielectric Bragg mirror. *Phys. Rev. B* **76**, 165415 (2007).
35 ME Sasin, et al., Tamm plasmon polaritons: Slow and spatially compact light. *Appl. Phys. Lett.* **92**, 251112 (2008).
36 O Gazzano, et al., Evidence for Confined Tamm Plasmon Modes under Metallic Microdisks and Application to the Control of Spontaneous Optical Emission. *Phys. Rev. Lett.* **107**, 247402 (2011).
37 G Lheureux, et al., Polarization-Controlled Confined Tamm Plasmon Lasers. *ACS Photonics* **2**, 842–848 (2015).
38 R Brückner, et al., Phase-locked coherent modes in a patterned metal–organic microcavity. *Nat. Photonics* **6**, 322–326 (2012).
39 L Ferrier, et al., Tamm plasmon photonic crystals: From bandgap engineering to defect cavity. *APL Photonics* **4**, 106101 (2019).
40 PN Melentiev, et al., Single nanohole and photonic crystal: wavelength selective enhanced transmission of light. *Opt. Express* **19**, 22743 (2011).
41 IV Treshin, VV Klimov, PN Melentiev, VI Balykin, Optical Tamm state and extraordinary light transmission through a nanoaperture. *Phys. Rev. A* **88**, 023832 (2013).
42 Y Zhan, DY Lei, X Li, SA Maier, Plasmonic fano resonances in nanohole quadrumers for ultra-sensitive refractive index sensing. *Nanoscale* **6**, 4705–4715 (2014).
43 WL Barnes, WA Murray, J Dintinger, E Devaux, TW Ebbesen, Surface Plasmon Polaritons and Their Role in the Enhanced Transmission of Light through Periodic Arrays of Subwavelength Holes in a Metal Film. *Phys. Rev. Lett.* **92**, 107401 (2004).
44 JA Hutchison, DM O'Carroll, T Schwartz, C Genet, TW Ebbesen, Absorption-Induced Transparency. *Angewandte Chemie Int. Ed.* **50**, 2085–2089 (2011).
45 JA Schuller, et al., Plasmonics for extreme light concentration and manipulation. *Nat. Mater.* **9**, 193–204 (2010).
46 AM Shrivastav, U Cvelbar, I Abdulhalim, A comprehensive review on plasmonic-based biosensors used in viral diagnostics. *Commun. Biol.* **4**, 70 (2021).
47 E Mauriz, Recent Progress in Plasmonic Biosensing Schemes for Virus Detection. *Sensors* **20**, 4745 (2020).
48 AA Yanik, et al., An Optofluidic Nanoplasmonic Biosensor for Direct Detection of Live Viruses from Biological Media. *Nano Lett.* **10**, 4962–4969 (2010).
49 A Li, X Wang, L Guo, S Li, Tunable Subradiant Mode in Free-Standing Metallic Nanohole Arrays for High-Performance Plasmofluidic Sensing. *J. Phys. Chem. C* **123**, 25394–25401 (2019).
50 AN Koya, et al., Novel Plasmonic Nanocavities for Optical Trapping-Assisted Biosensing Applications. *Adv. Opt. Mater.* **8**, 1901481 (2020).
51 T Yoshikawa, M Tamura, S Tokonami, T Iida, Optical Trap-Mediated High-Sensitivity Nanohole Array Biosensors with Random Nanospikes. *J. Phys. Chem. Lett.* **8**, 370–374 (2017).
52 CSH Hwang, Ms Ahn, KH Jeong, Extraordinary sensitivity enhancement of Ag-Au alloy nanohole arrays for label-free detection of Escherichia Coli. *Biomed. Opt. Express* **12**, 2734–2743 (2021).
53 IG Balasa, et al., Double-Langmuir model for optimized nanohole array-based plasmonic biosensors. *Appl. Surf. Sci.* **556**, 149802 (2021).
54 X Li, et al., Plasmonic nanohole array biosensor for label-free and real-time analysis of live cell secretion. *Lab Chip* **17**, 2208–2217 (2017).
55 H Im, et al., Template-Stripped Smooth Ag Nanohole Arrays with Silica Shells for Surface Plasmon Resonance Biosensing. *ACS Nano* **5**, 6244–6253 (2011).
56 C Liu, V Kamaev, ZV Vardeny, Efficiency enhancement of an organic light-emitting diode with a cathode forming two-dimensional periodic hole array. *Appl. Phys. Lett.* **86**, 143501 (2005).
57 M Kang, L Guo, Nanoimprinted Semitransparent Metal Electrodes and Their Application in Organic Light-Emitting Diodes. *Adv. Mater.* **19**, 1391–1396 (2007).
58 O Hess, et al., Active nanoplasmonic metamaterials. *Nat. materials* **11**, 573–584 (2012).
59 DJ Bergman, MI Stockman, Surface Plasmon Amplification by Stimulated Emission of Radiation: Quantum Generation of Coherent Surface Plasmons in Nanosystems. *Phys. Rev. Lett.* **90**, 027402 (2003).

60 MI Stockman, Spasers explained. *Nat. Photonics* **2**, 327–329 (2008).
61 Fv Beijnum, et al., Surface Plasmon Lasing Observed in Metal Hole Arrays. *Phys. Rev. Lett.* **110**, 206802 (2013).
62 DS Hecht, L Hu, G Irvin, Emerging Transparent Electrodes Based on Thin Films of Carbon Nanotubes, Graphene, and Metallic Nanostructures. *Adv. Mater.* **23**, 1482–1513 (2011).
63 N Kwon, K Kim, S Sung, I Yi, I Chung, Highly conductive and transparent Ag honeycomb mesh fabricated using a monolayer of polystyrene spheres. *Nanotechnology* **24**, 235205 (2013).
64 HA Atwater, A Polman, Plasmonics for improved photovoltaic devices. *Nat. Mater.* **9**, 205–213 (2010).
65 X Zhang, Q Huang, J Hu, RJ Knize, Y Lu, Hybrid tandem solar cell enhanced by a metallic hole-array as the intermediate electrode. *Opt. Express* **22**, A1400 (2014).
66 K Mashooq, MA Talukder, Management of light absorption in extraordinary optical transmission based ultra-thin-film tandem solar cells. *J. Appl. Phys.* **119**, 193101 (2016).
67 T Thio, KM Pellerin, RA Linke, HJ Lezec, TW Ebbesen, Enhanced light transmission through a single subwavelength aperture. *Opt. Lett.* **26**, 1972–1974 (2001).
68 J Rivas, C Schotsch, P Haring Bolívar, H Kurz, Enhanced transmission of thz radiation through subwavelength holes. *Phys. Rev. B* **68**, 201306 (2003).
69 A Forouzmand, AB Yakovlev, Tunable dual-band subwavelength imaging with a wire medium slab loaded with nanostructured graphene metasurfaces. *AIP Adv.* **5**, 077108 (2015).
70 F Miyamaru, et al., Terahertz surface-wave resonant sensor with a metal hole array. *Opt. letters* **31 8**, 1118–20 (2006).
71 GP Papari, C Koral, A Andreone, Geometrical dependence on the onset of surface plasmon polaritons in thz grid metasurfaces. *Sci. Reports* **9**, 924 (2019).
72 M Sun, et al., A photonic switch based on a hybrid combination of metallic nanoholes and phase-change vanadium dioxide. *Sci. Reports* **8**, 11106 (2018).
73 J Federici, Review of terahertz and subterahertz wireless communications. *J. Appl. Phys.* **107**, 111101–111101 (2010).
74 IF Akyildiz, JM Jornet, C Han, Terahertz band: Next frontier for wireless communications. *Phys. Commun.* **12**, 16–32 (2014).
75 T Otsuji, et al., Emission and detection of terahertz radiation using two-dimensional electrons in iii–v semiconductors and graphene. *IEEE Transactions on Terahertz Sci. Technol.* **3**, 63–71 (2013).
76 AC Ferrari, et al., Science and technology roadmap for graphene, related two-dimensional crystals, and hybrid systems. *Nanoscale* **7**, 4598–4810 (2015).
77 JM Jornet, N Thawdar, E Woo, MAA III, Temporal dynamics of frequency-tunable graphene-based plasmonic grating structures for ultra-broadband terahertz communication in *Disruptive Technologies in Sensors and Sensor Systems*, eds. RD Hall, M Blowers, J Williams. (International Society for Optics and Photonics, SPIE), Vol. 10206, pp. 41 – 51 (2017).
78 A De Leebeeck, et al., On-Chip Surface-Based Detection with Nanohole Arrays. *Anal. Chem.* **79**, 4094–4100 (2007).
79 H Im, JN Sutherland, JA Maynard, SH Oh, Nanohole-Based Surface Plasmon Resonance Instruments with Improved Spectral Resolution Quantify a Broad Range of Antibody-Ligand Binding Kinetics. *Anal. Chem.* **84**, 1941–1947 (2012).
80 A Lesuffleur, H Im, NC Lindquist, KS Lim, SH Oh, Laser-illuminated nanohole arrays for multiplex plasmonic microarray sensing. *Opt. Express* **16**, 219–224 (2008).
81 FJ Garcia-Vidal, L Martín-Moreno, JB Pendry, Surfaces with holes in them: new plasmonic metamaterials. *J. Opt. A: Pure Appl. Opt.* **7**, S97–S101 (2005).
82 X Wang, H Wang, Self-assembled nitride–metal nanocomposites: recent progress and future prospects. *Nanoscale* **12**, 20564–20579 (2020).